MPV reduction using Al III–calix[4]arene Lewis acid catalysts: Molecular-level insight into effect of ketone binding

Partha Nandi [a], Yuriy I. Matvieiev [b], Vyacheslav I. Boyko [b], Kathleen A. Durkin [c], Vitaly I. Kalchenko [b], Alexander Katz [a,*]

[a] Department of Chemical and Biomolecular Engineering, University of California, Berkeley, CA 94720, United States
[b] Institute of Organic Chemistry, National Academy of Sciences of Ukraine, Murmanska Str. 5, 02660 Kyiv-94, Ukraine
[c] College of Chemistry, University of California, Berkeley, CA 94720-1462, United States

ARTICLE INFO

ABSTRACT

Catalytic Meerwein–Ponndorf–Verley (MPV) reduction using Al III–calix[4]arene complexes is investigated as a model system that requires the bringing together of two different chemical species, ketone and alkoxide, within a six-membered transition state. Two-point versus one-point ketone binding is demonstrated to be the most salient feature that controls MPV catalysis rate. A 7.7-fold increase in rate is observed when comparing reactants consisting of a bidentate Cl-containing ketone and sterically and electronically similar but looser-binding ketones, which are substituted with H and F. The one-point and two-point nature of ketone binding for the various ketones investigated is independently assessed using a combination of structural data derived from single-crystal X-ray diffraction and DFT-based molecular modeling. Using MPV catalysis with inherently chiral calix[4]arenes, the effect of multiple point reactant binding on enantioselectivity is elucidated. A higher denticity of ketone binding appears to increase the sensitivity of the interplay between chiral active site structure and MPV reduction enantioselectivity.

1. Introduction

The rigid juxtapositioning of reactants is generally thought to be one of the crucial effects used by enzymes to achieve high rate enhancements and enantioselectivities and underlies induced-fit theories of enzyme action, which hinge on the precise geometric alignment of electronic orbitals between two reacting moieties within the transition state [1]. The kinetic consequences of juxtapositioning two reactive centers have been investigated in early synthetic model systems consisting of intramolecular cyclization reactions [2]. These systems demonstrate rate enhancements of up to 10^4 upon reactive functional group rigidification [3] and, therefore, provide insight into transition-state structure via reactant ground-state effects.

A lofty goal in the synthesis of bioinspired catalysts is to demonstrate the effect of rigid juxtapositioning of reactants on kinetics and enantioselectivity of a functioning catalytic active site. It is commonly believed that increasing rigidity or reactant preorganization in a catalyst lends itself to higher rates. This has been difficult to rigorously prove because of the general complexity of catalytic systems and the difficulty of experimentally deconvoluting chemical effects such as electronics and sterics from the mechanical effects having to do with the rigidity of reactant juxtapositioning. For example, Crabtree et al. [4] compare Ir-based imine formation catalysts with and without an aromatic R–NH$_2$ substituent. Catalyst containing this substituent is shown to result in a 30% rate increase and is hypothesized to activate the carbonyl carbon by acting as a hydrogen bond donor while also increasing aldehyde reactant binding denticity. The deconvolution of the latter two effects, consisting of reactant binding rigidification and differences in electrophilicity of reacting functional groups, on reaction rate could not be performed in this case. Another example involves antibody catalysts for the Diels–Alder reaction [5], which reveal a four-fold higher catalyzed rate constant and 40-fold higher binding affinity for the mature versus germ-line active site. However, even when using computational modeling of the active site, it has been difficult to deconvolute and single out the effect of rigidity of reactant juxtapositioning alone, presumably due to the complex and cooperative nature of interactions at the active site [6]. In this manuscript, our objective is to rigorously investigate the kinetic consequences of increased rigidity of reactant juxtapositioning in a functioning catalyst active site. Our approach uses the MPV reduction as catalyzed by Al III–calix[4]arene complexes, which covalently bind the Al III metal center in a bidentate configuration and within an oxo environment. The steric bulk of the calixarene as ligand enforces site isolation and the concept of a discrete active site by disfavoring the formation of aggregates, as observed in related Lewis acid catalysts [7]. Previous investigators have observed increased rate of MPV reduction catalysis when using more

* Corresponding author. Fax: +1 510 642 4778.
E-mail address: askatz@berkeley.edu (A. Katz).

sterically bulky ligands (i.e., either methyl or ethyl *ortho*-disubstituted BINOL ligands relative to BINOL) [8].

The MPV reduction reaction requires the preorganization of alkoxide and ketone as schematically represented in Fig. 1 [9]. When using the Al[III]-catalyzed MPV reduction as a model reaction, there appears to be a heretofore unexplained trend in the literature: higher rates are observed for reactants possessing halogen substituents in either the *ortho* or alpha position. In 1986, Hössegen et al. considered the MPV reduction of 1,3-conjugated imines in pyrimidinones using Al(O[i]Pr)₃ as catalyst [10]. Their data demonstrate a 65% conversion when a Cl substituent is in the 3 position, whereas the substitution of Cl with H yields a reactant that undergoes no reaction under identical conditions. In 2001, Maruoka et al. performed the MPV reduction in various aryl ketones. When a Cl substituent is either *ortho* or alpha to the carbonyl substituent, a significant increase in the rate of MPV catalysis was observed, in some instances being more than 3.5-fold [11]. In 2007, Nguyen et al. performed an elegant comparative study of MPV reduction enantioselectivity using BINOL-derived catalysts and both α-bromoacetophenone and acetophenone as reactants. Their catalytic rate data demonstrate a five-fold faster MPV reduction for α-bromoacetophenone relative to acetophenone. In the same study, Nguyen et al. showed that α-bromoacetophenone possessed uniformly higher enantioselectivity during reduction for a series of selective catalysts, relative to acetophenone, and this was attributed to two-point binding of the ketone via Br···Al as well as carbonyl···Al interactions [8]. This study inspired us, in this manuscript, to perform a comparative investigation for the effect of denticity of ketone binding on MPV reduction rate by deconvoluting.

Our approach begins with an investigation into how MPV reaction rate changes with calix[4]arene ligand substituents, hydride donor ability of the bound alkoxide via hyperconjugative stabilization, and electrophilicity of the ketone carbonyl carbon hydride acceptor. By comparing rates of sterically and electronically similar ketone reactants using the same Al[III]–calix[4]arene complex as catalyst active site, we elucidate the kinetic consequences of tighter two-point versus one-point binding of ketone on MPV reaction rate, shown in Fig. 1. To independently support two-point versus one-point ketone binding to the Al[III] center, we use structural data derived from single-crystal X-ray diffraction of molecular complexes and DFT to model ketone binding to the metal catalyst in model Al[III]-based active sites. We also investigate the repercussions of increased denticity of ketone binding on MPV reduction enantioselectivity when using inherently chiral calix[4]arene diols [12] as diastereomeric ligands for the Al(III)-based Lewis acid catalyst active site. By investigating the dependence of MPV reaction enantioselectivity on calix[4]arene diastereomer for both rigidly binding and looser-binding ketones, we elucidate the interplay between tightness of reactant juxtapositioning and enantioselectivity differences between the two diastereomers as catalysts.

2. Results and discussion

2.1. Calixarene catalyst design and synthesis

The goal of our ligand design approach is to enforce site isolation of Al[III] cations, since this has been previously observed to increase the rate of MPV catalysis [13]. Our strategy relies on using calix[4]arenes as bulky ligands, which have been previously demonstrated to enforce site isolation of metal clusters and cations [14–18]. Use of a calix[4]arene ligand also provides an organizational scaffold for tuning catalyst activity and selectivity via substituents and inherent chirality.

Previously reported Al[III]–calix[4]arene complexes in the literature [19,20] either do not have a hydride donating alkoxy group or are coordinatively saturated and thus disfavor isopropoxide
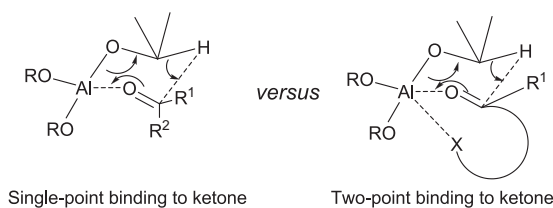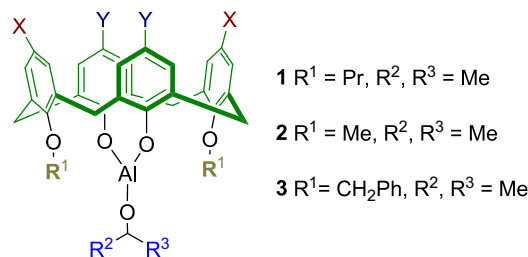

Fig. 1. Conceptual illustration of the central comparison being investigated in this study: effect of two-point versus single-point ketone binding on the rate of direct hydride transfer during MPV reduction. The substituent X can be a functional group that interacts with the Lewis acid center, such as Cl, as shown in this manuscript.

Scheme 1. Design of calix[4]arene-based ligands for Al[III] catalysis of the MPV reaction.

formation from alcohol in solution. Our design relies on bis-alkoxy calix[4]arenes as bidentate phenolate ligands for Al[III], which facilitates the formation of a vacant coordination site for isopropanol binding on the Al[III] center, as represented by **1** in Scheme 1. Although 1,3-dimethoxy calix[4]arene **2** also chelates to Al[III], unlike **1**, which exhibits exclusively cone conformer upon Al[III] binding, complex **2** shows a 1:1 mixture of cone and partial cone conformations via ¹H NMR spectroscopy in d⁸-toluene. This conformational mobility is likely due to the small size of the methyl substituent at the lower rim, which allows free rotation of aromatic rings through the macrocycle annulus [21]. As in **1**, a lack of conformational mobility is also observed when using sterically bulky benzyl substituents in **3**.

²⁷Al NMR spectroscopy is a sensitive probe of isolated Al[III] active sites in solution, since it is possible to characterize differences between aggregated octahedral Al species and isolated trigonal planar/tetrahedral sites [22]. ²⁷Al NMR spectroscopic data shown in Fig. 2b demonstrate a single resonance for catalyst **1** in toluene solution at 71 ppm – corresponding to a tetrahedral site. A tetrahedral site could be consistent with either (i) datively coordinating calixarene lower-rim alkoxy substituents to a monomeric Al metal center, since this type of dative coordination involving calixarene lower-rim alkoxy substituents is observed in similar metal–calix[4]arene complexes [19], (ii) datively coordinating alcohol to a monomeric Al Lewis acid site, or (iii) an alkoxide-bound μ²-oxo dimer as the relevant solution species. Trigonal and octahedral sites are expected to yield resonances at 110 ppm and 0 ppm, respectively. A control consisting of a freshly prepared airfree solution of aluminum isopropoxide in the absence of calix[4]arene ligand exhibits multiple resonances observed at 71 ppm and 0 ppm, which indicates higher coordination organometallic complexes even at initial time. These two resonances increase in intensity upon air-free storage, and a new resonance at 25 ppm appears that represents penta-coordinate Al(III) sites [18], as shown in Fig. 2a. These data demonstrate the critical function of the calix[4]arene ligand in limiting the aggregation of Lewis acid sites into higher oligomers in solution. This presumably arises due to the role of the calix[4]arene as a sterically bulky entity, as shown previously for grafted surface complexes [7,14–16].
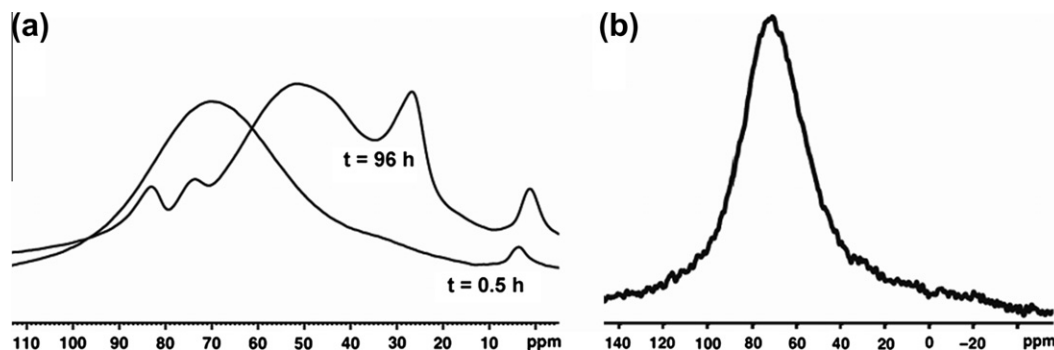
Fig. 2. (a) ^{27}Al NMR of an airfree mixture consisting of Al(O^{i}Pr)$_3$ freshly prepared from AlMe$_3$ + 3 equiv. of 2-propanol in toluene at initial time (t = 0.5 h) and at t = 96 h after synthesis, and (b) ^{27}Al NMR of **1** in toluene. Spectrum in (b) does not change during the course of 96 h after synthesis.

Table 1
Representative substrate scope of MPV reduction with aluminum calix[4]arene.

Substrate	Product		Yield
			90
			75
			71[a]
			80
			74
			72
			85[a]
			55
			60
			80

[a] Refers to isolated yield rather than GC yield. All reactions are conducted in (~5 mL) toluene at room temperature for a duration of 12 h using 10 mol% catalyst **1**, 4 equiv. alcohol, and 1 mmol ketone.

2.2. Kinetic isotope effect and substrate scope

Ratner et al. have carefully investigated the mechanism of Al^{III}-catalyzed MPV reactions using a combined experimental and DFT-based computational approach. Their results correlate a large primary kinetic isotope effect (KIE) for MPV reduction of acetophenone using isopropanol, which they measured to be 2.3, with a direct mechanism of hydride transfer [23]. This mechanism involves a six-membered chair transition state in which hydride transfer occurs as shown in Fig. 1 [24,25]. Using the reduction of α-chloroacetophenone with isopropanol in toluene at room temperature, a KIE of 3.0 is measured for catalyst **1**. This large KIE measured for the MPV reduction reaction [18] implies that breakage of the isopropyl C–H bond is the rate determining step over others, such as alcoholysis [26,27]. Such a result is consistent with the direct hydride transfer mechanism [19,20].

The versatility of catalytic MPV reduction using **1** as catalyst is demonstrated in Table 1. The reaction tolerates aryl groups, halogens, and cyclopropyl groups, which is similar to previously reported MPV catalysts [28]. For 4-phenyl-cyclohexanone, the reduction yields a mixture of diastereomers where the cis/trans ratio is 1:3 (detected by ^{1}H NMR spectroscopy). This is similar to the diastereoselectivity previously reported for an Al^{III} catalyst based on 2-hydroxy-2′-(perfluorooctanesulfonylamino)biphenyl ligand and means that the hydride delivery preferentially occurs from a sterically more constrained axial approach, which favors the formation of the thermodynamically stable trans alcohol product [11]. Data in Table 1 indicate that catalyst **1** exhibits catalytic turnover, and we have demonstrated a zero-order dependence of rate on ketone concentration (see Supporting information). Both of these data are consistent with previously reported MPV reduction catalysts [8,11].

2.3. Effect of calix[4]arene catalyst on MPV reaction rate

A comparative study of the effect of various calix[4]arene substituents and alkoxide hydride donors on catalysis is shown in Table 2. The primary objective of these studies is to elucidate the role of sterics in the immediate vicinity of the active site so as to investigate the possibility of a cavity enveloping the active site and defined by calix[4]arene lower-rim substituents R^1. Entries **1–3** demonstrate a two-fold slower rate for bulky isopropyl over n-propyl substituents and a decrease of ~23% for benzyl versus n-propyl substituents. The latter is interesting given that benzyl and n-propyl substituents should sterically behave similarly, given almost identical E_s values according to Taft's equation [29], and suggests that enthalpically favorable cation-π interactions between calix[4]arene substituent phenyl groups and the Al center may enforce a more rigid and confined cavity, as defined by the space between lower-rim substituents, in **3**.

Table 2 demonstrates hyperconjugative effects at the hydride donating α-carbon for the MPV reaction, as well the effect of electron-withdrawing groups at the calix[4]arene upper rim. A primary alkoxide substituent donates hydride to a much weaker extent than

Table 2
Systematic comparison of structure and activity of aluminum calix[4]arene mediated MPV reduction.

.
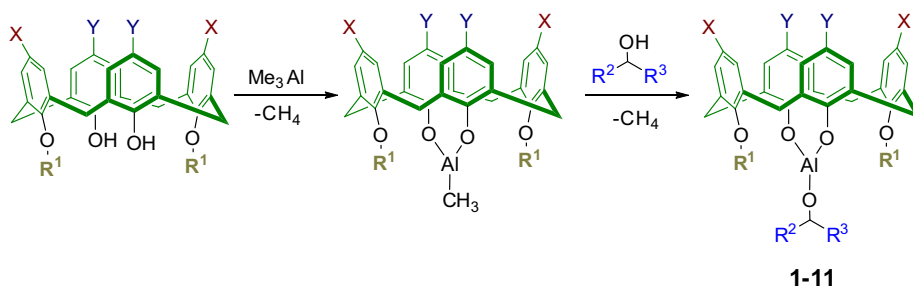
Catalyst	R_1	R_2	R_3	X	Y	Rel. rate
1	**$CH_2CH_2CH_3$**	CH_3	CH_3	$(CH_3)_3C$	$(CH_3)_3C$	1
2	**$CH(CH_3)_2$**	CH_3	CH_3	$(CH_3)_3C$	$(CH_3)_3C$	0.5
3	**CH_2Ph**	CH_3	CH_3	$(CH_3)_3C$	$(CH_3)_3C$	0.8
4	$CH_2CH_2CH_3$	**CH_2CH_3**	**CH_3**	$(CH_3)_3C$	$(CH_3)_3C$	1
5	$CH_2CH_2CH_3$	***Ph***	**CH_3**	$(CH_3)_3C$	$(CH_3)_3C$	1.6
6	$CH_2CH_2CH_3$	***2-Nph***	**H**	$(CH_3)_3C$	$(CH_3)_3C$	0.5
7	$CH_2CH_2CH_3$	***2-Nph***	**CH_3**	$(CH_3)_3C$	$(CH_3)_3C$	1.3
8	$CH_2CH_2CH_3$	***Ph***	***Ph***	$(CH_3)_3C$	$(CH_3)_3C$	1.7
9	$CH_2CH_2CH_3$	CH_3	CH_3	**H**	**H**	1.4
10	$CH_2CH_2CH_3$	CH_3	CH_3	**$(CH_3)_3C$**	**NO_2**	0.4
11	$CH_2CH_2CH_3$	CH_3	CH_3	**$(CH_3)_3C$**	**$P(O)Ph_2$**	N.R.

All reactions were run at room temperature in anhydrous toluene (~5 mL) with 10 mol% catalyst, 4 equiv. alcohols (R_2R_3CHOH), and 1 mmol 2-chloroacetophenone. N.R. = no reaction.

a secondary alkoxide when comparing both **1** and **7** to **6**. This suggests a greater degree of hyperconjugative stabilization of the ensuing carbocation upon hydride delivery for the secondary alkoxide and is consistent with the observed 2.6-fold faster rate for **7** relative to **6**, as well as a 1.7-fold faster rate for **8** relative to **1**. A smaller effect of hyperconjugative stabilization is observed when comparing phenyl and methyl substituents in **8** versus **5**, respectively, which is consistent with a reproducibly 6% faster rate for **8**. A relevant control for hyperconjugative effects in Table 2 is the lack of observed change in hyperconjugative stabilization when comparing methyl and ethyl substituents in **1** and **4**, respectively. Consistent with trends predicted by Hammet constants for increasing Lewis acidity at the Al metal center, a slightly stronger Lewis acid results upon changing calix[4]arene upper-rim substituent from *tert*-butyl (**1**) to H (**9**). Stronger Lewis acidity has been previously implicated in a 14-fold enhanced MPV rate when using dual carbonyl activation, as enforced by two Al centers at the active site, when compared to a single Al center catalyst [25]. This trend of increased Lewis acidity at the active site resulting in catalytic MPV rate enhancement is not upheld for the nitro and phosphine-oxide upper-rim substituents in **10** and **11**, respectively, presumably due to substituent coordination to the Al metal center. Also presumably due to coordination of N, O, and Cl functional groups to the Al metal center, attempts to measure the Hammett ρ value for the MPV reaction are unsuccessful when using *para*-substituted benzhydrols (similar to **8** except with *para* substituents of benzhydrol being NMe_2, OMe, or Cl).
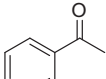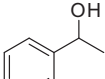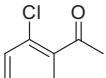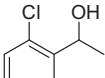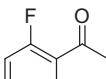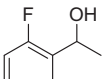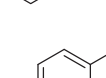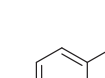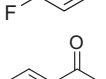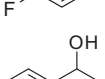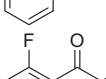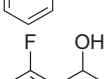
2.4. Effect of ketone on MPV reaction rate

Table 3 summarizes initial reaction rates (calculated at less than 15% ketone conversion) for the MPV reduction of ketones of varying electrophilicity at the α-carbon and size, when using catalyst **1**. When comparing chlorine, fluorine, and hydrogen substituents on acetophenone, there is a 7.7-fold higher rate in entry **2** relative to entries **1** and **3** in Table 3. This difference in rate is unlikely to be

due to changes in the electrophilicity of the carbonyl carbon because the similar pK_a values for the corresponding *para*-substituted H, F, and Cl benzoic acids demonstrate a lack of direct correlation with rate (i.e., H = 4.19, F = 4.14, Cl = 3.98) [30]. Changing the substituent to be an sp^3 Cl in entry **5** results in a more than 10-fold higher rate relative to entries **1** and **3** in Table 3. This could be due to a stronger two-point binding involving the sp^3-hybridized halogen to the Al center as well as the possibility of increased electrophilicity of the carbonyl carbon. The effect of the latter on reactivity can be observed by compar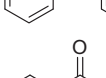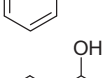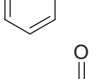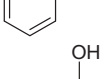ing entries **5** and **8** in Table 3. The substitution of H for a more electron-withdrawing Cl substituent on the α-carbon leads to a 40% rate enhancement of entry **8** over entry **5**. Altogether, the observations above suggest that while electrophilicity of the carbonyl carbon also contributes to a higher MPV reaction rate, the dominant effect appears to be presence of a Cl in proximity to the ketone carbonyl.

Later we investigate whether differences in denticity of ketone binding may be expected between ketones with F and Cl substituents in proximity to the carbonyl. Although we are unable to obtain a single-crystal structure of catalyst **1** bound with ketone substrate, which could possibly show two-point binding to the substrate (e.g., entries **2**, **5** or **8** in Table 3), there is abundant evidence for Al···Cl–C(sp^3) coordination [31] as well as Al···Cl–C(sp^2) coordination in the crystallography literature [32]. However, evidence for similarly strong Al···F–C(sp^3) and Al···F–C(sp^2) interactions [33] could not be found. Further support for stronger metal···Cl interactions that are possible in entries **2**, **5**, and **8** in Table 3 versus metal···F interactions that are possible in entries **3**, **4**, and **6** in Table 3 is provided by data in Table 4. Table 4 consists of metal···halogen X-ray crystallographic bond distances in structures that consist of both covalently bound fluorine and chlorine substituents. In all of these structures in Table 4, the intermolecular metal···halogen bond distance contraction for chlorine is significantly shorter than the corresponding contractions for fluorine. This means that Al···Cl interactions are stronger than

Table 3
Rate comparison of ketone reactants in MPV reaction with 1,3-bis-propoxy-calix[4]arene aluminum (catalyst **1** in Table 2) catalyst.

Entry	Substrate	Product	C.L.	TOF (h^{-1})
1	(acetophenone)	(1-phenylethanol)	2.52	0.44
2	(2'-chloroacetophenone)	(1-(2-chlorophenyl)ethanol)	3.1	3.42
3	(2'-fluoroacetophenone)	(1-(2-fluorophenyl)ethanol)	2.51	0.44
4	(4'-fluoroacetophenone)	(1-(4-fluorophenyl)ethanol)	2.51	0.28
5	(2-chloroacetophenone)	(2-chloro-1-phenylethanol)	2.9	4.7
6	(2-fluorobenzophenone)	(2-fluorobenzhydrol)	5.7	0.22
7	(valerophenone)	(1-phenylpentanol)	5.3	0.2
8	(2,2-dichloroacetophenone)	(2,2-dichloro-1-phenylethanol)	2.49	6.62

All reactions were run in anhydrous toluene (~5 mL) at room temperature with 10 mol% catalyst loading, 4 mmol of 2-propanol, and with 1 mmol of ketone substrate. C.L. – characteristic length.

rather than using the full-blown Al^{III}–calix[4]arene complex. This model consists of Al isoproxide derived from (Z)-ethene-1,2-diol and successfully captures the rigidity of the calix[4]arene diol as ligand without encumbering additional computational cost. Both the model (Z)-ethene-1,2-diol ligand as well as the calix[4]arene-based ligands provide a similarly open site for accommodating two-point ketone binding as ascertained from force-field molecular modeling. Similar two-point ketone binding has been invoked using other types of rigid and sterically bulky diols based on substituted BINOL ligands [8]. Ketone substrates corresponding to entries **1**, **2**, and **3** from Table 3 are bound to the active site. In all cases, the calculations confirm that the hydride transfer transition state is cyclic and consists of a chair-like six-membered ring assembly. In the case of ketone in entry **2**, the transition-state Al···Cl distance is 3.4 Å, which is shorter than the van der Waals distance of 3.8 Å and is indicative of a non-bonding Al···Cl interaction. This non-bonding interaction is also observed in an earlier stage of the reaction coordinate and can be termed as a precomplex. In stark contrast, Al···H and Al···F non-bonding interactions and precomplex formation were not observed in the case of ketones corresponding to entries **1** and **3**, respectively, in Table 3. In addition, the force constants associated with the transition-state vector are significantly larger for the case of ketone in entry **2** relative to entries **1** and **3** in Table 3. This indicates a tighter and more rigid transition state for ketone in entry **2** [35].

We propose that the observed rate difference in catalytic rate trends in entries **1**, **2**, and **3** of Table 3 is controlled by the denticity of ketone attachment to the Al metal center. This relies on a correlation between the mechanical rigidity of ketone and alkoxide juxtapositioning in the transition state and hydride transfer rate during MPV catalysis. Such a correlation is qualitatively consistent with the decreased likelihood of α-carbon substituents interfering with hydride transfer in the concerted chair-like six-membered transition state. The motion of these substituents could otherwise cause unfavorable distortions in the geometry of the activated complex (i.e., unfavorable 1,3-diaxial interactions between sterically bulky substituents). This effect of strong two-point binding hypothesized previously elucidates previous observations of higher Al^{III}-catalyzed MPV rates for reactants possessing Cl substituents in either the ortho or alpha position [11]. It is also consistent with trends observed in intramolecular reaction systems [2], which show greater rates upon more rigid degrees of preferentially organizing two reacting moieties. The effect of two-point binding observed here is also qualitatively consistent with comparative studies of mature and germ-line catalytic antibodies for the Diels–Alder reaction. This reaction requires the bringing together of two reactants in the transition state and shows a fourfold higher rate for the mature relative to germ-line antibody. Our results here support the hypothesis that it is the greater rigidity of the mature antibody in bringing the two reactants together, relative to the germline, that accounts for the rate difference. This greater rigidity is reflected in a 40-fold higher binding constant for the reactants in the mature versus germ-line antibody [5].

A final observation from data in Table 3 involves the interplay between sizes of ketone and the loosely defined calix[4]arene

Al···F interactions according to data in Table 4. Such Al···Cl interactions are also observed in other Al Lewis acid sites [34], including a weak Al Lewis acid site consisting of alkyl ligands in a dimeric structure, which is coordinated to a chloride anion [34b]. The data above require that a covalently bound chlorine substituent be a much better Lewis base than a fluorine substituent. Such a conclusion is intuitively reinforced by the greater elemental electronegativity of fluorine relative to chlorine. Based on the above, we suggest: (i) dative Al···Cl–C(sp^2) coordination to result in a two-point binding of chloroketone for ketone in entries **2** and **5** of Table 3, as schematically illustrated in Fig. 1, and (ii) fluoroketones in entries **3**, **4**, and **6** of Table 3 to bind to the Al center in a weaker attachment relative to chloroketone, and in a configuration that more resembles one-point binding in Fig. 1.

DFT calculations [34] are performed in order to gain further insight into the trends in Al···halogen interactions described previously. A model Al catalyst is used to simplify calculations

Table 4
Examples of non-covalent M···Cl and M···F contact distances from the literature.

RCl	R′F	M	M···F[a]	M···F–R′	$\Delta M···F$[b]	M···Cl[a]	M···Cl–R	$\Delta M···Cl$[b]
PhCl	[B(C$_6$F$_5$)$_4$]$^-$	Al^{III} [32]	3.52	3.23	**0.26**	3.80	2.54	**1.26**
ClCH$_2$Cl	[Ti(OTeF$_5$)$_6$]$^-$	Ag^I [38]	3.23	3.03	**0.20**	3.51	2.66	**0.95**
C$_6$Cl$_5$	N/A	Rh^{III} [39]	N/A	N/A	**N/A**	3.38	2.63	**0.75**

[a] Established van der Waals metal–halogen bond distances.
[b] Contraction distance due to metal–halogen non-covalent interactions.

cavity in the space between lower-rim substituents of **1**. This cavity size is calculated to have a characteristic radius of 2.7 Å for **1** via MM2 force-field molecular modeling. The effect of calix[4]arene cavity size is likely responsible for the two-fold rate difference when comparing catalysts **1** and **2** for the same reactants in Table 2. The effect of the calix[4]arene cavity of **1** is also investigated using differently sized reactants. The characteristic length defines the ketone reactant size (C.L. in Table 3) using an MM2 force-field calculation and corresponds to the energy-minimized distance between the carbonyl O and the smaller substituent adjacent to the carbonyl (e.g., in entry **2**, this is the $O\cdots CH_3$ distance of 3.1 Å). The C.L. is related to the energetic cost of ketone penetration into the cleft defined by calix[4]arene lower-rim substituents upon binding, with larger values of C.L. requiring higher energetic barrier. Comparison of larger ketones in entries **6** and **7** to the electronically similar entry **1** in Table 3 shows a two-fold lower rate for the larger ketones, which is likely due to sterics.

2.5. Asymmetric induction with inherently chiral calix[4]arenes

We use inherently chiral calix[4]arene catalysts **12** and **13** as shown in Scheme 2, to investigate the repercussions of higher denticity of ketone binding in a system that exhibits enantioselectivity in MPV reduction. Chirality in calix[4]arenes **12** and **13** is derived from two primary effects: (i) an asymmetric *AB*-type substitution on the calix[4]arene lower rim, which serves as a macrocyclic scaffold for appending asymmetry via a chiral substitution pattern (directionality), and (ii) an asymmetric carbon center of the phenylethylamine substituent. Chirality arising from the latter effect is transferred diffusely throughout the calix[4]arene skeleton [36]. Both of these effects are expected to contribute to asymmetric induction in catalyzed processes when using **12** and **13** as catalysts, based on previous investigations [37]. There are two relevant control experiments pertaining to this aspect. First, when using a chiral catalyst that is synthesized by treating trimethyl aluminum with excess chiral alcohol (R)-(−)-2-methyl-butanol in toluene, a lack of any product enantioselectivity is observed for α-chloroacetophenone as reactant. Second, when using **12** as catalyst and isopropanol as reductant, no enantioselectivity is observed during reduction of α-chloroacetophenone. Optically pure aluminum complexes **12** and **13** are readily synthesized in three steps starting from the monomethoxycalix[4]arene as shown in Scheme 2. The first step is the regioselective proximal alkylation of monomethoxy-*p-tert*-butyl calix[4]arene using a twofold excess of (*S*)-*N*-(α-phenylethyl)bromoacetamide in NaOH/DMSO, followed by silica column chromatographic separation of the diastereomers formed using hexane/ethylacetate 4:1 in accordance with the literature [7]. The second step is the reaction of the diastereomers with
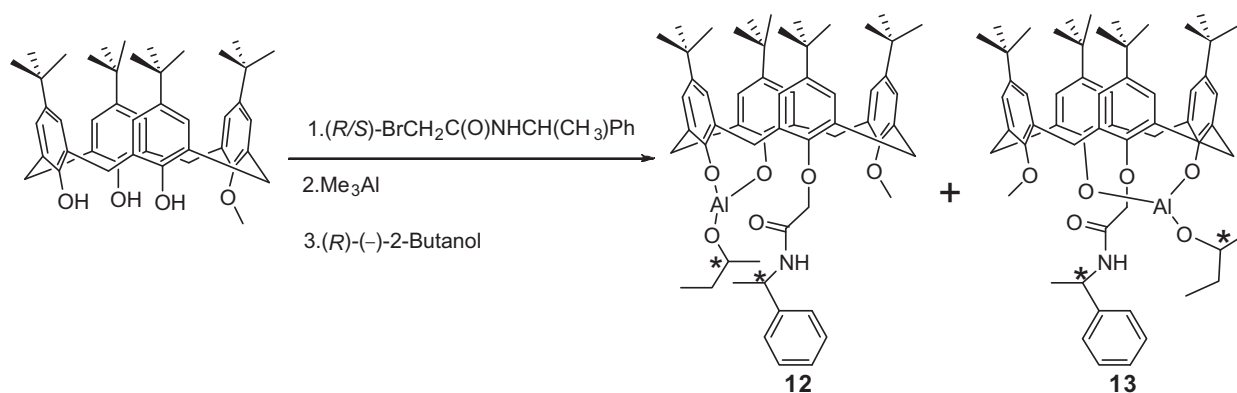
Table 5
Results of enantioselective MPV reduction using catalysts **12** and **13**.

Reactant	Product	ee **12**	ee **13**	TOF (h^{-1})
(phenacyl chloride)	(2-chloro-1-phenylethanol)	10	19	4.6[a]
(2-fluorobenzophenone)	(2-fluorobenzhydrol)	20	20	0.54[a]
(2-chloroacetophenone)	(1-(2-chlorophenyl)ethanol)	4	12	3.2[a]
(acetophenone)	(1-phenylethanol)	ND[b]	ND[b]	0.48[a]

All reactions were run in anhydrous toluene (∼5 mL) at room temperature with 10 mol% catalyst loading, 10 mmol of (R)-(−)-2-methyl-butanol, and with 1 mmol of ketone substrate. Percent enantiomeric excess is represented by ee.
[a] Measured at ∼10% conversion.
[b] ND means that ee was ≤2%.

Me_3Al, and the last step is the alcoholysis reaction of the Me−Al complexes with (R)-(−)-2-butanol.

We have previously demonstrated a quantitative interdependence between increasing degree of rigidity and increasing degree of chirality transfer on the length scale of a calix[4]arene skeleton. Here, we use this interdependence as an indirect probe of denticity of coordination for bound reactants at the aluminum center in catalysts **12** and **13**. Our hypothesis is that the difference in inherent chirality between **12** and **13** should most influence the enantioselectivity of a reaction with a rigid transition state. Based on our results above, this in turn requires that the MPV enantioselectivity should be more sensitive to the inherent chirality differences between **12** and **13** when using a ketone molecule that binds in a two-point configuration to the aluminum metal center than when using a one-point binding ketone.

Results in Table 5 demonstrate MPV reduction of four reactants, α-chloroacetophenone, *ortho*-chloroacetophenone, *ortho*-fluorobenzophenone, and acetophonone using R-(−)-2-methyl-butanol as hydride source. As a control experiment, in the absence of a chiral calixarene ligand, when using catalyst **1**, no enantioselectivity is observed. Enantioselectivity remains at 20% independent of which calix[4]arene diastereomer **12** and **13** is used as ligand when using *ortho*-fluorobenzophenone. In stark contrast, the MPV

1.(R/S)-BrCH₂C(O)NHCH(CH₃)Ph

2.Me₃Al

3.(R)-(−)-2-Butanol

12 + **13**

Scheme 2. Synthesis of inherently chiral calix[4]arene catalysts **12** and **13**.

enantioselectivity sensitively depends on the calix[4]arene inherent chirality when using α-chloroacetophenone and changes from 10% for **12** to 19% for **13** in Table 5. The observed enantioselectivity with α-chloroacetophenone in this experiment is in stark contrast to the lack of enantioselectivity for the same ketone in the control experiments described previously. Altogether, these results emphasize the importance of cooperativity between normal chirality arising from the alcohol and inherent chirality arising from the calixarene scaffold in these experiments. Cooperativity between normal and inherent chirality was previously shown to be critical for asymmetric induction by Matt and coworkers, for alkylation and hydrogenation reactions [39]. MPV enantioselectivity is also sensitive to calix[4]arene inherent chirality when using *ortho*-chloroacetophenone and changes from 4% for **12** to 12% for **13** in Table 5. The observed several-fold rate increase for the Cl-containing ketones over F-containing ketone in Table 5 is consistent with the expected tighter binding of the former, though this cannot be rigorously deconvoluted from electronic and steric factors, which also contribute to the rate difference. Results shown in Table 5 demonstrate acetophenone to be an unselective reactant from the standpoint of enantioselectivity. As such, it is insensitive to chirality within catalysts **12** and **13** and provides no useful information regarding the correlation between rigidity of ketone binding and sensitivity of enantioselectivity to the particular catalyst diastereomer used. The results in Table 5 demonstrate that the sensitivity of the interplay between MPV enantioselectivity and chirality in the ligand increase upon increasingly rigid reactant juxtapositioning. They also demonstrate the absolute enantioselectivity need not increase upon increasingly rigid reactant juxtapositioning (i.e., comparison of entries for α-chloroacetophenone and *ortho*-chloroacetophenone with *ortho*-fluorobenzophenone in Table 5).

3. Conclusion

Catalyst and reactant structural requirements for MPV reduction have been elucidated in a system involving Al^{III}–calix[4]arene complexes as active sites. The calix[4]arene provides an oxo environment that covalently binds to the aluminum center in a bidentate configuration and acts as an organizational scaffold at the active site, which permits the design and synthetic tuning of catalyst structure. The large kinetic isotope effect measured with calix[4]arene catalysts suggests hydride transfer to be the rate-limiting step in the reaction. A comparative approach is used for deconvoluting electronic and steric effects at the active site for MPV reduction catalysis. Reactant electronic effects are understood on the basis of increasing the electrophilicity of the carbonyl carbon of the ketone, which results in a better hydride acceptor, as well as increasing hydride donor ability of the bound alkoxide derived from the alcohol via hyperconjugative stabilization. In addition, there is a 40% increase in MPV catalysis rate upon increasing the Lewis acidity of the metal center via changing calix[4]arene upper-rim substituents from *tert*-butyl to less electron donating H. Steric considerations accounting for the effect of a cavity formed by calix[4]arene lower-rim substituents result in a factor of two lower reaction rate when using either sterically demanding calix[4]arene substituents or bulky reactants. This result suggests formation of a shape-selective cavity that is defined by lower-rim substituents.

The most crucial feature that affects MPV reaction rate is the two-point versus one-point binding of ketone reactant to the Lewis acid site. This effect alone leads to a 7.7-fold higher rate during MPV catalysis favoring the more rigid two-point binding ketone. The denticity of ketone binding is independently investigated using DFT-based calculations. The above correlation between

MPV catalysis rate and ketone and alkoxide juxtapositioning at the active site is consistent with trends observed in intramolecular reaction systems [2], as well as comparative studies of mature and germ-line catalytic antibodies for reactions requiring the bringing together of two reactants in the transition state [5]. The repercussions of two-point versus one-point ketone binding on enantioselective MPV catalysis are also investigated using inherently chiral calix[4]arenes. Increasing denticity of ketone reactant binding is observed to increase the sensitivity of the interplay between inherently direction of inherent chirality in the calixarene ligand and MPV reaction enantioselectivity.

4. Experimental procedure

General procedure for conducting MPV reduction: In 5 mL of anhydrous toluene (freshly distilled over sodium benzophenone ketyl), 1,3-bis-substituted calix[4]arene (e.g., for 1,3-bispropoxy calix[4]arene, 73 mg, 0.1 mmol, 10 mol%) is dissolved. To this solution, Me₃Al (40 µL, 0.1 mmol, 10 mol%, 25% w/w solution in hexane) is added under Ar. Gaseous methane bubbles indicate the formation of methylaluminum calix[4]arene complex, which upon treatment with alcohol forms the active MPV catalyst and evolves methane. A 5 mL solution of alcohol (e.g., 300 µL, 240 mg, 4 mmol, 4 equiv. anhydrous 2-propanol) and substrate ketone (e.g., 155 mg, 1 mmol, 1 equiv. α-chloroacetophenone) in toluene is added. The reaction is subsequently performed at room temperature and is monitored by ¹H NMR spectroscopy.

Appendix A. Supplementary material

Supplementary data associated with this article can be found, in the online version, at doi:10.1016/j.jcat.2011.08.013.

References

[1] A. Radzicka, R. Wolfenden, Science 267 (1995) 90.
[2] (a) A.J. Kirby, Adv. Phys. Org. Chem. 29 (1994) 87;
    (b) D.E. Storm, D.E. Koshland Jr., Proc. Natl. Acad. Sci. USA 66 (1970) 445.
[3] T.C. Bruice, F.C. Lightstone, Acc. Chem. Res. 32 (1999) 127.
[4] D.-H. Lee, R.H. Crabtree, S.-K. Park, Bull. Korean Chem. Soc. 23 (2002) 1157.
[5] (a) F.E. Romesberg, B. Spiller, P.G. Schultz, R.C. Stevens, Science 279 (1998) 1929;
    (b) X. Zhang, Q. Deng, S.H. Yoo, K.N. Houk, J. Org. Chem. 67 (2002) 9043;
    (c) A. Heine, E.A. Stura, J.T. Yli-Kauhaluoma, C. Gao, Q. Deng, B.R. Beno, K.N. Houk, K.D. Janda, I.A. Wilson, Science 279 (1998) 1934;
    (d) J. Zimmermannn, F.E. Romesberg, C.L. Brooks, I.F. Thorpe, J. Phys. Chem. B 114 (2010) 7359;
    (e) A. Piatesi, D. Hilvert, ChemBioChem 5 (2004) 460;
    (f) D. Hilvert, K.W. Will, K.D. Nared, M.-T.M. Auditor, J. Am. Chem. Soc. 111 (1989) 9261;
    (g) L.T. Chong, Y. Duan, L. Wang, I. Massova, P.A. Kollman, Proc. Natl. Acad. Sci. USA 96 (1999) 14330.
[6] S. Marti, J. Andres, V. Moliner, E. Silla, I. Tuñón, J. Bertrán, Chem. Eur. J. 14 (2008) 596.
[7] (a) N. de Silva, S.J. Hwang, K.A. Durkin, A. Katz, Chem. Mater. 21 (2009) 1852;
    (b) J.M. Notestein, E. Iglesia, A. Katz, J. Am. Chem. Soc. 126 (2004) 16478.
[8] C.R. Graves, H. Zhou, C.L. Stern, S.T. Nguyen, J. Org. Chem. 72 (2007) 9121.
[9] (a) For recent reviews on MPV reduction see: C.F. de Graauw, J.A. Peters, H. van Bekkum, J. Huskens, Synthesis (1994) 1007;
    (b) J.S. Cha, Org. Process Res. Dev. 10 (2006) 1032;
    (c) C.R. Graves, J.E. Campbell, S.T. Nguyen, Tetrahedron: Asymmetry 16 (2005) 3460;

(d) K. Nishide, M. Node, Chirality 14 (2002) 759;
(e) T. Ooi, T. Miura, Y. Itagaki, H. Ichikawa, K. Maruoka, Synthesis (2002) 279.

[10] T. Höseggen, F. Rise, K. Undheim, J. Chem. Soc. Perkin Trans. 1 (1986) 849.

[11] T. Ooi, H. Ichikawa, K. Maruoka, Angew. Chem. Int. Ed. 40 (2001) 3610; T. Ooi, H. Ichikawa, K. Maruoka, Angew. Chem. 113 (2001) 3722.

[12] M.A. Kliachyna, O.A. Yesypenko, V.V. Pirozhenko, S.V. Shishkina, O.V. Shishkin, V.I. Boyoko, V.I. Kalchenko, Tetrahedron 65 (2009) 7085.

[13] (a) R. Kow, R. Nygren, M.W. Rathke, J. Org. Chem. 42 (1977) 826;
(b) E.J. Campbell, H. Zhou, S.T. Nguyen, Org. Lett. 3 (2001) 2391.

[14] N. de Silva, J.-M. Ha, A. Solovyov, M.M. Nigra, I. Ogino, S.W. Yeh, K.A. Durkin, A. Katz, Nat. Chem. 2 (2010) 1062.

[15] J.-M. Ha, A. Solovyov, A. Katz, Langmuir 25 (2009) 10548.

[16] A. Katz, P.D. Costa, A.C.P. Lam, J.M. Notestein, Chem. Mater. 14 (2002) 3364.

[17] J.M. Notestein, A. Solovyov, L.R. Andrini, F.G. Requejo, A. Katz, E. Iglesia, J. Am. Chem. Soc. 129 (2007) 15585.

[18] J.M. Notestein, L.R. Andrini, V.I. Kalchenko, F.G. Requejo, A. Katz, E. Iglesia, J. Am. Chem. Soc. 129 (2007) 1122.

[19] J.L. Atwood, S.G. Bott, C. Jones, C.L. Raston, J. Chem. Soc. Chem. Commun. (1992) 1349.

[20] V.C. Gibson, C. Redshaw, W. Clegg, M.R.J. Elsegood, Polyhedron 16 (1997) 4385.

[21] C.D. Gutsche, Calixarenes: An Introduction, Monographs in Supramolecular Chemistry, Royal Society of Chemistry, Cambridge, 2008.

[22] J.W. Akitt, in: J. Mason (Ed.), Multinuclear NMR, Plenum Press, NY, 1988, p. 259 (Chapter 9).

[23] R. Cohen, C.R. Graves, S.T. Nguyen, J.M.L. Martin, M.A. Ratner, J. Am. Chem. Soc. 126 (2004) 14796.

[24] R.B. Woodward, N.L. Wendler, F.J. Brutschy, J. Am. Chem. Soc. 67 (1945) 1425.

[25] L.M. Jackman, J.A. Mills, Nature 164 (1949) 789.

[26] V.J. Shiner, D. Whittaker, J. Am. Chem. Soc. 85 (1963) 2337.

[27] W.N. Moulton, R.E. van Atta, R.R. Ruch, J. Org. Chem. 26 (1961) 290.

[28] (a) T. Ooi, T. Miura, K. Maruoka, Angew. Chem. Int. Ed. 37 (1998) 2347; Angew. Chem. 110 (1998) 2524;
(b) K. Maruoka, Bull. Chem. Soc. Jpn. 82 (2009) 917;
(c) E.J. Campbell, H. Zhou, S.T. Nguyen, Angew. Chem. Int. Ed. 41 (2002) 1020; Angew Chem. 114 (2002) 1062;
(d) A. Corma, M.E. Domine, L. Nemeth, S. Valencia, J. Am. Chem. Soc. 124 (2002) 3194;
(e) A. Corma, M.E. Domine, S. Valencia, J. Catal. 215 (2003) 294.

[29] R.W. Taft Jr., J. Am. Chem. Soc. 74 (1952) 2729.

[30] C.A. Hollingsworth, P.G. Seybold, C.M. Hadad, Int. J. Quant. Chem. 90 (2002) 1396.

[31] H.C. Brown, W.J. Wallace, J. Am. Chem. Soc. 75 (1953) 6279.

[32] A.V. Korolev, F. Delpech, S. Dagorne, I.A. Guzei, R.F. Jordan, Organometallics 20 (2001) 3367.

[33] T. Belgardt, J. Storre, H.W. Roesky, M. Noltemeyer, H.-G. Schmidt, Inorg. Chem. 34 (1995) 3821.

[34] (a) D.M. Van Seggen, P.K. Hurlburt, O.P. Anderson, S.H. Strauss, J. Am. Chem. Soc. 114 (1992) 10995;
(b) D. Zhang, Eur. J. Inorg. Chem. (2007) 3077.

[35] M.P. Garcia, M.V. Jimenez, A. Cuesta, C. Siurana, L.A. Oro, F.J. Lahoz, J.A. Lopez, M.P. Catalan, A. Tiripicchio, M. Lanfranchi, Organometallics 16 (1997) 1026.

[36] Calcuations are optimized using Gaussian 09 (Revision B.01) by M.J. Frisch et al., the ωB97X-D functional, and the 6-311++G(d,p) basis set. This approach has been previously shown to have less error than the B3LYP series for subtle nonbonded effects, as relevant in this study. See J.-D. Chai, M. Head-Gordon, Phys. Chem. Chem. Phys. 10 (2008) 6615 and Supporting information.

[37] Details of these calculations can be found in the Supporting information.

[38] A. Solovyov, J.M. Notestein, K.A. Durkin, A. Katz, New J. Chem. 32 (2008) 1314.

[39] C. Dieleman, S. Steyer, C. Jeunesse, D. Matt, J. Chem. Soc. Dalton Trans. (2001) 2508.